Superlattices and Microstructures, Vol. 28, No. 3, 2000
doi:10.1006/spmi.2000.0902
Available online at http://www.idealibrary.com on IDEAL

Reflectivity modeling of Si-based amorphous superlattices

E. L. ZEBALLOS-VELÁSQUEZ, H. MONCADA L.
Faculdad de Ciencias Físicas, Universidad Nacional Mayor de San Marco, Ciudad Universitaria s/n, Lima, Peru

M. C. A. FANTINI†
Instituto de Física, Universidade de Säo Paulo, Caixa Postal 66318, 05315-970 Säo Paulo, SP, Brazil

(Received 13 January 2000)

The structural properties of superlattices composed by hydrogenated amorphous silicon/silicon carbide (a-Si:H/a-$Si_{1-x}C_x$:H) and silicon/germanium (a-Si:H/a-Ge:H), deposited by the plasma-enhanced chemical vapor deposition (PECVD) technique, were analyzed by means of small-angle X-ray diffraction. The relevant structural parameters, such as the multilayer period, the individual layer thickness, the width of the interface and the optical constants, were determined by modeling the experimental reflectivity. The model was based on the dynamical diffraction theory, including material mixing at the interface, interface roughness and random variation of component thickness. In addition, the effect of the direct beam and background on the measured intensities were considered.

Key words: Si amorphous superlattices, small angle X-ray diffraction

1. Introduction

Semiconductor superlattices prepared by many deposition techniques have attracted much attention during this decade; in particular, amorphous multilayers of a-Si:H/a-$Si_{1-x}C_x$:H and a-Si:H/a-Ge:H have deserved much research effort [1–3]. These systems, like many others, can be successfully obtained, for example, by the plasma-enhanced chemical vapor deposition (PECVD) method, also named glow discharge [3, 4] and ion-beam sputtering [5], which is used in electronic and optical devices, solar cells and other applications [6–8].

The small-angle X-ray diffraction (SAXRD) technique has been well explored in order to provide information about the structural quality of amorphous multilayers, since wide-angle diffraction is not suitable to characterize these systems.

Our earlier work [9, 10] dealt with the experimental results on the structure of a-Si:H/a-$Si_{1-x}C_x$:H and a-Si:H/a-Ge:H multilayers, prepared by PECVD, where some of the relevant structural parameters were determined. Nevertheless, only one a-Si:H/a-Ge:H sample [10] was taken as an example for theoretical modeling, where different defects were considered and their contributions to the diffracted intensity were separated. In this case we analyzed the best obtained multilayer, regarding its SAXRD characterization.

In this work, we present the experimental reflectivity modeling of all deposited and analyzed Si-based multilayers, using the same modeling procedure. As settled earlier, the simulations of the experimental data

†Author to whom correspondence should be addressed. E-mail: mfantini@if.usp.br

0749–6036/00/090207 + 09 $35.00/0

Table 1: Thickness of the individual layers, interface, and period obtained from the fitting of the SAXRD experimental data of the a-Si:H/a-$Si_{1-x}C_x$:H and a-Si:H/a-Ge:H multilayers.

SAMPLE	d_{Si}(Å)	d_{SiC}(Å)	d_{Ge}(Å)	d_{int}(Å)	d(Å)
M80/2	70	70		6	146
M80/3	95	73		6	174
M80/4	163	80		8	251
134	132		94	16	242
135	112		70	16	198
137	58		29	16	103
138	31		14	16	61
141	17		7	12	36

Table 2: Real component of the optical constants of the amorphous phases obtained from the fitting of the SAXRD experimental data of the a-Si:H/a-$Si_{1-x}C_x$:H and a-Si:H/a-Ge:H multilayers.

SAMPLE	$\delta_{Si}(10^{-6})$	$\delta_{SiC}(10^{-6})$	$\delta_{Ge}(10^{-6})$	$\delta_{int}(10^{-6})$
M80/2	9.94	9.15		9.70
M80/3	8.59	8.09		8.17
M80/4	9.04	7.97		8.67
134	7.10		9.66	7.22
135	7.38		9.87	8.26
137	5.14		9.82	7.35
138	5.26		9.79	7.15
141	8.58		11.0	9.19

Table 3: Imaginary component of the optical constants of the amorphous phases obtained from the fitting of the SAXRD experimental data of the a-Si:H/a-$Si_{1-x}C_x$:H and a-Si:H/a-Ge:H multilayers.

SAMPLE	$\beta_{Si}(10^{-7})$	$\beta_{SiC}(10^{-7})$	$\beta_{Ge}(10^{-7})$	$\beta_{int}(10^{-7})$
M80/2	9.99	9.52		9.76
M80/3	9.92	9.81		9.85
M80/4	9.96	9.20		9.76
134	9.50		9.98	9.87
135	5.78		9.84	6.37
137	9.75		9.98	9.87
138	9.13		9.91	9.79
141	6.77		8.99	7.89

Table 4: Estimated values of the mean roughness (r) and period variation (Δd) obtained from the fitting of the SAXRD experimental data of the a-Si:H/a-$Si_{1-x}C_x$:H and a-Si:H/a-Ge:H multilayers.

SAMPLE	r(Å)	$\pm\Delta d$(Å)
M80/2	8.0	4.0
M80/3	6.0	3.0
M80/4	8.0	4.0
134	11.0	6.0
135	12.0	4.0
137	9.0	5.0
138		5.0
141		3.0

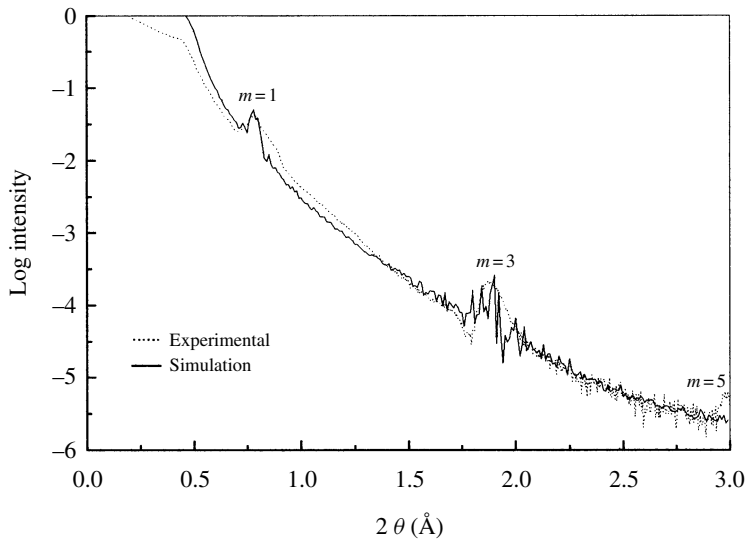

Fig. 1. Experimental and simulation results of the small-angle X-ray diffraction reflectivity of sample M80/2 (a-Si:H/a-$Si_{1-x}C_x$:H).

were combined with a fitting process from which the amorphous component's parameters are obtained, for example, thickness and the X-ray optical constants.

2. Experimental

The detailed sample's growth PECVD process are described elsewhere [9–11]. For both types of samples, gaseous mixtures of SiH_4, either with CH_4 or GeH_4 inside the glow discharge chamber, were used. The layers were deposited on glass substrate, alternating periodically the gas composition inside the reactor.

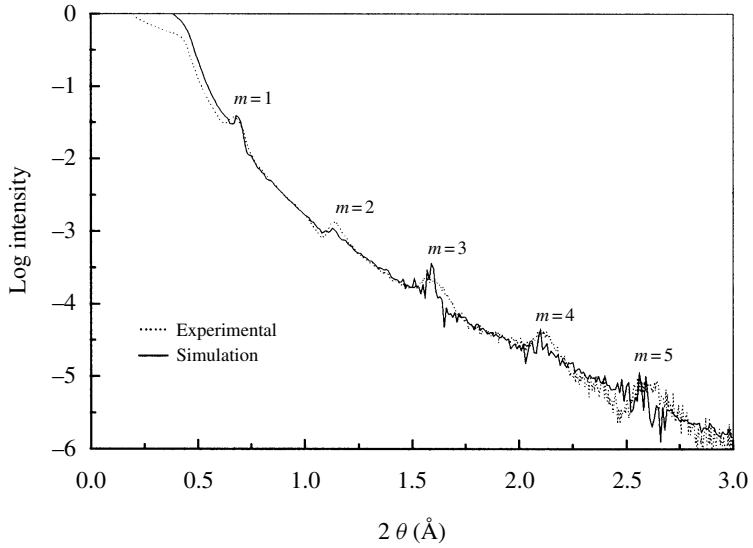

Fig. 2. Experimental and simulation results of the small-angle X-ray diffraction reflectivity of sample M80/3 (a-Si:H/a-$Si_{1-x}C_x$:H).

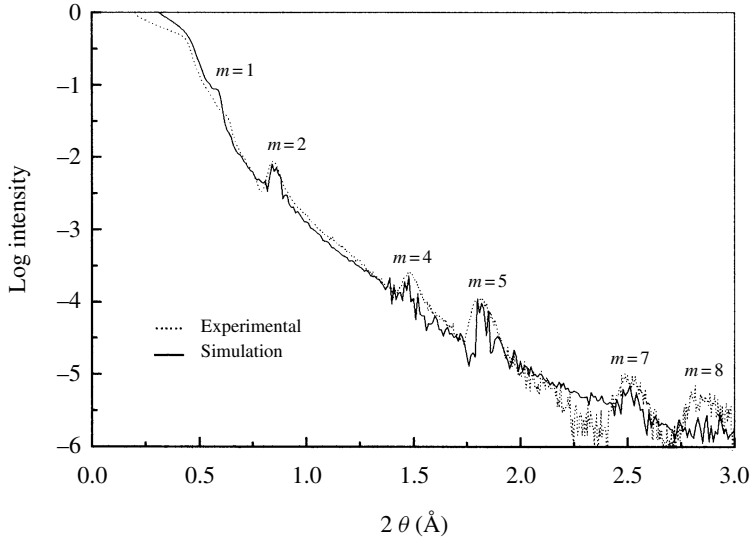

Fig. 3. Experimental and simulation results of the small-angle X-ray diffraction reflectivity of sample M80/4 (a-Si:H/a-$Si_{1-x}C_x$:H).

The SAXRD measurements were performed in a conventional X-ray diffractometer, with a θ–2θ geometry, using step scanning mode and monochromatized Cu Kα radiation ($\lambda = 0.15418$ nm). The 2θ values varied from 0.2 ° to 6.0 °.

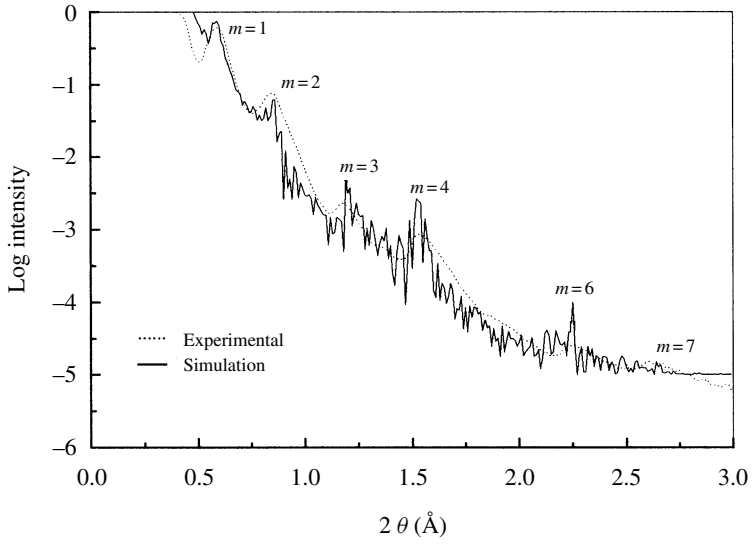

Fig. 4. Experimental and simulation results of the small-angle X-ray diffraction reflectivity of sample 134 (a-Si:H/a-Ge:H).

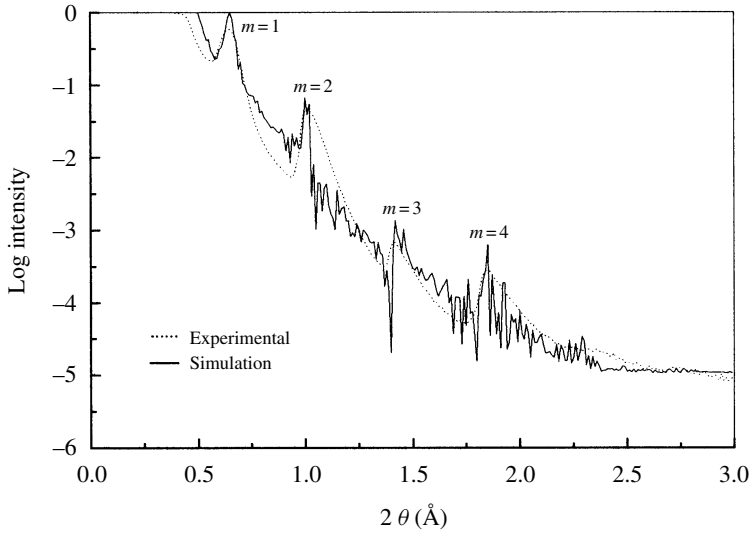

Fig. 5. Experimental and simulation results of the small-angle X-ray diffraction reflectivity of sample 135 (a-Si:H/a-Ge:H).

3. Results

The theoretical reflectivity model of the multilayers was based on Fresnel's coefficients, including absorption. The X-ray refractive index of each A or B material that composes the system is given by [12, 13]:

$$\eta = 1 - \delta - i\beta, \tag{1}$$

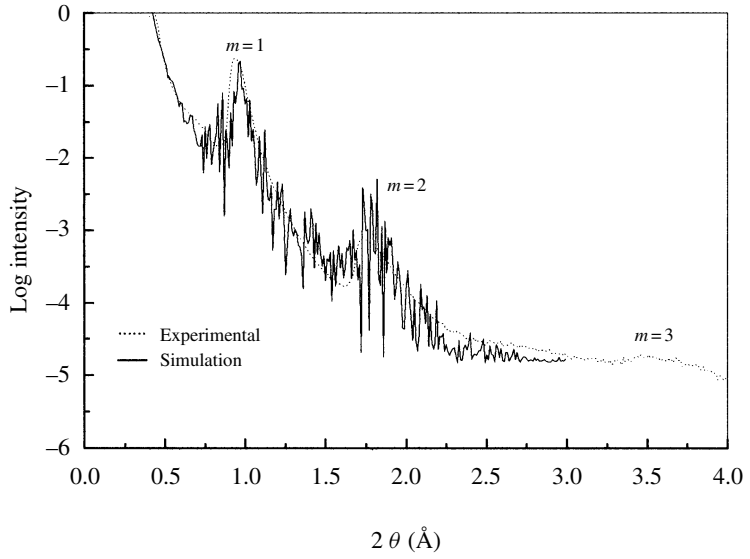

Fig. 6. Experimental and simulation results of the small-angle X-ray diffraction reflectivity of sample 137 (a-Si:H/a-Ge:H).

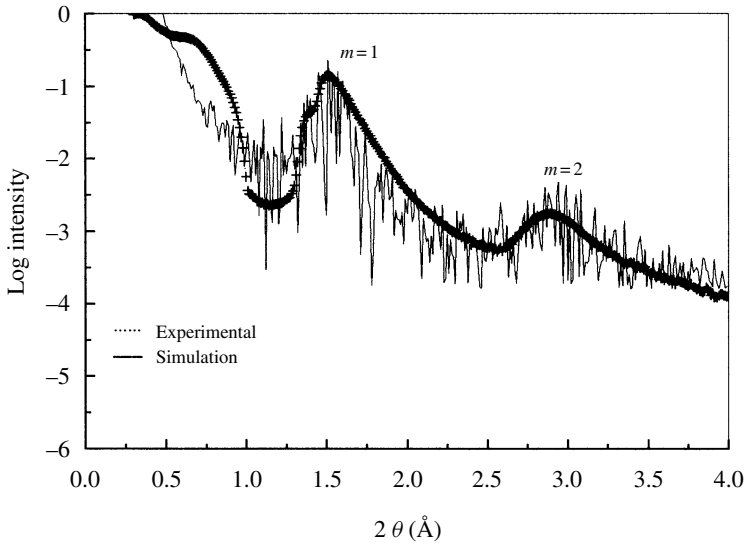

Fig. 7. Experimental and simulation results of the small-angle X-ray diffraction reflectivity of sample 138 (a-Si:H/a-Ge:H).

where δ and β are, respectively, the real and imaginary parts of the refractive index of each layer, which are calculated by [14–16]:

$$\delta = \frac{\aleph r_e \lambda^2}{2\pi}(Z + \Delta f') \qquad \text{and} \qquad \beta = \frac{\aleph r_e \lambda^2}{2\pi}(\Delta f'') = \frac{\mu\lambda}{4\pi}, \tag{2}$$

where λ is the wavelength, μ is the linear total absorption coefficient [14], Z is the atomic number, $\Delta f'$ is the real dispersion correction and $\Delta f''$ is the imaginary dispersion correction for each material considered.

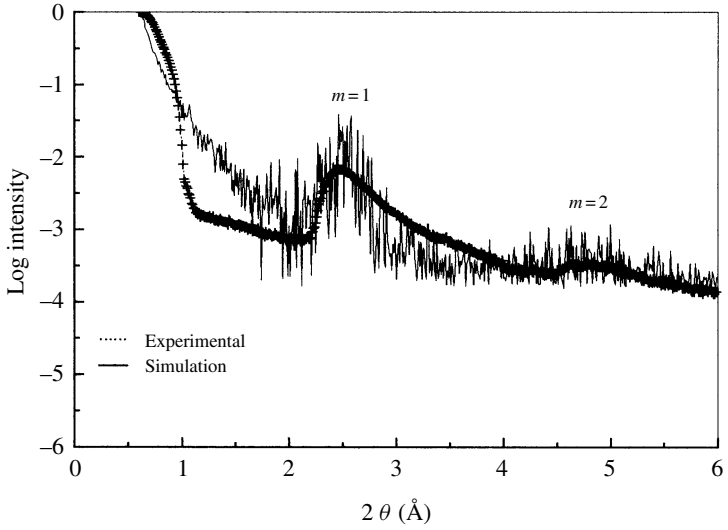

Fig. 8. Experimental and simulation results of the small-angle X-ray diffraction reflectivity of sample 141 (a-Si:H/a-Ge:H).

The δ value can vary up to 20%, depending on the values taken for $\Delta f'$ and $\Delta f''$ [17]. For a mixture of materials, like those of interfaces, the constants $\bar{\delta}$ and $\bar{\beta}$ are calculated using the relations:

$$\overline{\delta} = \frac{\lambda}{4\pi}\overline{\rho}\sum g_i\left(\frac{\mu}{\rho}\right)_i\left(\frac{Z_i + \Delta f_i'}{\Delta f_i''}\right) \qquad \text{and} \qquad \overline{\beta} = \frac{\lambda}{4\pi}\bar{\rho}\sum g_i\left(\frac{\mu}{\rho}\right)_i, \tag{3}$$

where $\bar{\rho}$ is the density of the mixture and g_i is the weight fraction of the constituents having a mass absorption coefficient of $\left(\frac{\mu}{\rho}\right)_i$ [17, 18].

The determination of the superlattice mean period (d) is obtained by means of the interference Bragg relation corrected by refraction [12, 13], assuming $\beta < \delta \ll 1$:

$$m\lambda = 2d\left[1 - \frac{\delta}{(\sin\theta_{\text{obs}})^2}\right](\sin\theta_{\text{obs}}), \tag{4}$$

where

$$\delta = \frac{\delta_{\text{A}} d_{\text{A}} + \delta_{\text{B}} d_{\text{B}}}{d_{\text{A}} + d_{\text{B}}} \tag{5}$$

and δ is a parameter given as a function of the refractive index (δ_{A}, δ_{B}) and thickness (d_{A}, d_{B}) of the individual layers [19].

Imperfections in the structure of the multilayers affect the intensity and width of the Bragg reflections, giving rise to differences between the experimental results and the theoretical calculations based on a perfect structure of multilayers. Non-abrupt interfaces, variations on the layer's thickness and interface roughness are the most common imperfections present in real multilayers. The size of the interface at which the refractive index of medium A, η_{A}, changes to that of medium B, η_{B}, is finite and can be evaluated by the fitting of the experimental spectrum. Also, imperfections due to deviations in the thickness of each layer affect the intensity of the diffraction peaks, as well as their width; these variations can be sequential or random. Finally, the substrate roughness and the deposition conditions can cause roughness on the surface of the deposited layers, affecting the structure of the lattice; this type of imperfection provokes X-ray scattering, decreasing the intensity of the reflections, and it can also be evaluated by the fitting of the experimental data.

The intensities of direct beam and background also have to be modeled in order to compare experimental and theoretical results. The simulation of the real structure combines all the above-mentioned effects.

In this work, the model for the simulation of the experimental reflectivity includes all the above-mentioned factors, separating their effects on the diffraction data. The interface is considered as a separate part of the structure, being a combination of both materials, with a thickness of d_{int} that can vary between certain limits. In the calculations of the hydrogenated amorphous silicon/silicon carbide structure the sequence of each period is a-$Si_{1-x}C_x$:H/interface/a-Si:H/interface, and in those of the hydrogenated amorphous silicon/germanium structure the sequence of each period is a-Si:H/interface/a-Ge:H/interface. In both cases we considered two layers of the material's mixture by period (interface A–B, material A, interface A–B, material B). In this model the roughness behaves as a Gaussian function and the variation in the thickness of each individual layer is random. In order to include this thickness variation (*VAR*) in the calculus, random numbers were generated by a congruent linear function given by [20]:

$$I_{j+1} = (aI_j + c) \bmod m, \tag{6}$$

where m is the period of the generator.

A sequence of random numbers is generated in the interval (0,1) [21] and, the thickness of each layer will present a fluctuation of $d_i \pm VAR$.

The thicknesses of each individual layer, as well as the period of the multilayers, from our previous works [9, 10], were used as the starting values for the present simulations. First, we considered in the model of three layers a fixed size for the interface, a Gaussian distribution of roughness and the effect of the direct beam and the background. From these fittings we obtained the thickness of each individual layer, the multilayer's period, the optical constants of the amorphous materials and the mean roughness, which varied from 6 to 12 Å. Fixing those values, the second step included the random variation in the layer's thickness, which gave values between 3 and 6 Å. Tables 1–4 and Figs 1–8 summarize the results obtained.

4. Discussion

By the evaluation of all obtained simulations one can verify that the experimental intensities are satisfactorily reproduced by the proposed model, particularly in the case of the high order reflections. This is due to the incorporation of different effects, all of them contributing to the experimental reflectivity results. For the samples studied, the large decrease in the intensity, mostly for the high orders, is due to the roughness of the interfaces, which begins at the substrate. The mean roughness of the a-Si:H/a-Ge:H samples grown on glass substrates is larger than the corresponding value of 5 Å, obtained for a similar multilayer on top of crystalline Si [10]. This result demonstrates once more the influence of the substrate on the structural quality of the multilayers. In the case of samples numbered 138 and 141, the roughness values could not be determined, since the diffraction peaks are very large; the increase in width is due to the fact that the size of the interface is very close to the thickness of the individual layers (see Table 1) .

The simulation results showed that the interface, being a mixture of both materials and a third layer in the structure, influences the relative intensity of the diffraction peaks. On the other hand, the random variation in the layer's thickness produces broad peaks with less intensity, making the experimental and theoretical results more similar. The incorporation of the direct beam and background contributions, as well as the optical constant values of the amorphous components, contributes to a better agreement between experimental and simulation data.

5. Conclusions

In this work we confirm our previous studies that indicated the necessity of inclusion of different structural inhomogeneities, such as material mixture, roughness and variations in periodicity, in order to obtain a fair

description of real multilayer structures. These effects are more evident when the interface's size is similar to the thicknesses of the multilayer's components. The roughness is independent of the period value, but produces a large decrease in the intensities, mostly in the high diffraction orders. The reflectivity modeling also established the necessity of a proper description of the effects caused by the direct beam and background, as well as the values of the amorphous material X-ray optical constants, not easily available by other experimental methods.

Acknowledgements—Thanks are due to Dr I. Pereyra for providing the silicon carbide multilayers and to Dr P. V. Santos for the germanium ones.

References

[1] P. D. Persans, A. F. Ruppert, B. Abeles, and T. Tiedje, Phys. Rev. **B32**, 5558 (1985).
[2] P. D. Persans, A. F. Ruppert, B. Abeles, G. Hughes, and K. S. Liang, Mater. Res. Soc. Symp. **149**, 711 (1989).
[3] P. V. Santos, M. Hundhausen, L. Ley, and C. Viczian, J. Appl. Phys. **69**, 778 (1991).
[4] J. Kakalios, H. Fritzche, N. Ibaraki, and S. R. Ovshinsky, J. Non-Cryst. Solids **66**, 339 (1984).
[5] S. M. Prokes and Spaepen, Appl. Phys. Lett. **47**, 234 (1985).
[6] H. Munekata and H. Kukimoto, Japan. J. Appl. Phys. **22**, L544 (1983).
[7] M. Yoshimoto, T. Fuyuki, and H. Matsunami, Japan. J. Appl. Phys. **25**, L922 (1986).
[8] S. Tsuda *et al*., Japan. J. Appl. Phys. **26**, 28 (1987).
[9] E. L. Z. Velasquez, M. C. A. Fantini, M. N. P. Carreño, I. Pereyra, H. Takahashi, and R. Landers, J. Appl. Phys. **75**, 543 (1994).
[10] E. L. Zeballos-Velásquez and M. C. A. Fantini, J. Non-Cryst. Solids **209**, 175 (1997).
[11] P. V. Santos and L. Ley, Phys. Rev. **B36**, 3325 (1987).
[12] B. Abeles and T. Tiedje, Phys. Rev. Lett. **51**, 2003 (1983).
[13] H. P. Klug and L. E. Alexander, *X-ray Diffraction Procedures for Polycrystalline and Amorphous Materials* (Wiley, New York, 1974).
[14] J. H. Underwood and T. W. Barbee, AIP Conf. Proc. **75**, 170 (1981).
[15] A. Guinier, *X-Ray Diffraction* (Freeman, London, 1963) p. 121.
[16] L. V. Azároff, *Elements of X-ray Crystallography* (McGraw-Hill, New York, 1968) p. 552.
[17] *International Tables for X-ray Crystallography* (International Union for Crystallography, Kynoch Press, Birmingham, UK, 1968) Vol. II, p. 194
[18] M. G. LeBoité, A. Traverse, L. Névot, B. Pardo, and J. Corno, J. Mater. Res. **3**, 1089 (1988).
[19] T. W. Barbee, Jr, AIP Conf. Proc. **75**, 131 (1981).
[20] D. Thomson, *Métodos Numéricos* (Pontifícia Universidade Católica de São Paulo, São Paulo, Brazil, 1995) 1st edn, 1st edn, p. 229
[21] W. Press, S. Teukosky, W. Vetterling, and B. Flannery, *Numerical Recipes in Fortran* (Cambridge University Press, UK, Cambridge, 1992) 2nd edn, p. 266, 2nd edn, p. 266